Although beams B and C are never separated in transverse position space, they are separated in transverse momentum space. The separation is $2\hbar k_{light}$, as is required for first-order Bragg reflection. Storing which-way information therefore corresponds to storing transverse momentum information with an accuracy of the order of $\Delta p_z \approx \hbar k_{light}$. So the uncertainty relation implies that the storing process must include a back action onto the transverse position of the order of $\Delta z \approx \lambda_{light}$. This back action is due to the following effect. In the Bragg regime, the interaction time with the standing light wave, t_{Bragg}, is so long that the atoms move at least a transverse distance of the order of $\lambda_{light}/2$ within t_{Bragg}. In a naive picture, the atoms can be Bragg-reflected at the beginning or at the end of this interaction, which implies a transverse position uncertainty of the order of $\Delta z \approx \lambda_{light}$. But this back action onto the near-field position cannot destroy the far-field fringe pattern. The interference pattern created in the interferometer is a pattern in momentum space, not in position space. The far-field position distribution is simply a picture of the final momentum distribution. □

Received 3 February; accepted 15 June 1998.

1. Bohr, N. in *Albert Einstein: Philosopher-Scientist* (ed. Schilpp, P. A.) 200–241 (Library of Living Philosophers, Evanston, 1949); reprinted in *Quantum Theory and Measurement* (eds Wheeler, J. A. & Zurek, W. H.) 9–49 (Princeton Univ. Press, 1983).
2. Feynman, R., Leighton, R. & Sands, M. in *The Feynman Lectures on Physics* Vol. III, Ch. I (Addison Wesley, Reading, 1965).
3. Scully, M. O., Englert, B. G. & Walther, H. Quantum optical tests of complementarity. *Nature* **351,** 111–116 (1991).
4. Haroche, S. in *High-resolution Laser Spectroscopy* (ed. Shimoda, K.) 253–313 (Topics in Applied Physics, Vol. 13, Springer, 1976).
5. Rauch, H. *et al.* Verification of coherent spinor rotation of fermions. *Phys. Lett. A* **54,** 425–427 (1975).
6. Badurek, G., Rauch, H. & Tuppinger, D. Neutron interferometric double-resonance experiment. *Phys. Rev. A* **34,** 2600–2608 (1986).
7. Storey, P., Tan, S., Collett, M. & Walls, D. Path detection and the uncertainty principle. *Nature* **367,** 626–628 (1994).
8. Englert, B. G., Scully, M. O. & Walther, H. Complementarity and uncertainty. *Nature* **375,** 367–368 (1995).
9. Storey, E. P., Tan, S. M., Collett, M. J. & Walls, D. F. Complementarity and uncertainty. *Nature* **375,** 368 (1995).
10. Wiseman, H. & Harrison, F. Uncertainty over complementarity? *Nature* **377,** 584 (1995).
11. Wiseman, H. M. *et al.* Nonlocal momentum transfer in welcher weg measurements. *Phys. Rev. A* **56,** 55–75 (1997).
12. Eichmann, U. *et al.* Young's interference experiment with light scattered from two atoms. *Phys. Rev. Lett.* **70,** 2359–2362 (1993).
13. Cohen-Tannoudji, C. Effect of non-resonant irradiation on atomic energy levels. *Metrologia* **13,** 161–166 (1977); reprinted in Cohen-Tannoudji, C. *Atoms in Electromagnetic Fields* 343–348 (World Scientific, London, 1994).
14. Kunze, S., Dürr, S. & Rempe, G. Bragg scattering of slow atoms from a standing light wave. *Europhys. Lett.* **34,** 343–348 (1996).
15. Kunze, S. *et al.* Standing wave diffraction with a beam of slow atoms. *J. Mod. Opt.* **44,** 1863–1881 (1997).
16. Bernhardt, A. F. & Shore, B. W. Coherent atomic deflection by resonant standing waves. *Phys. Rev. A* **23,** 1290–1301 (1981).

Acknowledgements. We thank S. Kunze for discussions. This work was supported by the Deutsche Forschungsgemeinschaft.

Correspondence and requests for materials should be addressed to G.R. (e-mail: gerhard.rempe@uni-konstanz.de).

A critical window for cooperation and competition among developing retinotectal synapses

Li I. Zhang*, Huizhong W. Tao*, Christine E. Holt†, William A. Harris† & Mu-ming Poo

Department of Biology, University of California at San Diego, La Jolla, California 92093-0357, USA
** These authors contributed equally to this work.*

In the developing frog visual system, topographic refinement of the retinotectal projection depends on electrical activity. *In vivo* whole-cell recording from developing *Xenopus* tectal neurons shows that convergent retinotectal synapses undergo activity-dependent cooperation and competition following correlated pre- and postsynaptic spiking within a narrow time window. Synaptic inputs activated repetitively within 20 ms before spiking of the tectal neuron become potentiated, whereas subthreshold inputs activated within 20 ms after spiking become depressed. Thus both the initial synaptic strength and the temporal order of activation are critical for heterosynaptic interactions among convergent synaptic inputs during activity-dependent refinement of developing neural networks.

Electrical activity in the developing nervous system plays a crucial role in the establishment of early nerve connections[1,2]. In the mammalian visual system, both the formation of ocular dominance columns in the primary visual cortex[3–5] and the segregation of retinal ganglion axons into eye-specific layers in the lateral geniculate nucleus[6] depend on electrical activity in the visual pathways. The pattern of activity in the optic nerves seems to serve an instructive role, as synchronous stimulation of optic nerves abolishes the formation of ocular dominance columns, whereas asynchronous stimulation leads to sharp ocular dominance columns[7]. Artificially synchronized activity in the optic nerve also disrupts the development of orientation tuning in the visual cortex[8]. In the visual system of frog, chick and fish, retinal axons use activity-independent mechanisms initially to establish a topographic map, but the initial map is coarse and terminals from each retinal axon arborize over a large portion of the tectum. During development, the map becomes refined as retinal axons progressively restrict their arborizations to a smaller fraction of the tectum[9,10]. Topographic refinement of the retinotectal projection also depends on activity patterns, as this process is impaired when retinal activity is blocked or uniformly synchronized by raising the animals in strobe light[11–14]. Thus, throughout the visual system, the refinement of connections depends on the pattern of activity, but the underlying physiological mechanisms are largely unknown.

We have examined quantitatively the effects of activity patterns on the strength of developing central synapses in the *Xenopus* retinotectal system. *In vivo* whole-cell recordings were made from neurons in the optic tectum of young *Xenopus* tadpoles to monitor changes in the strength of retinotectal synapses following repetitive electrical stimulation of retinal neurons in the contralateral eye. By

† Present address: Department of Anatomy, University of Cambridge, Cambridge CB2 3DY, UK.

studying an early stage of development, when each retinal ganglion cell axon innervates a large population of tectal cells, we were able to examine the role of activity in both cooperative and competitive interactions among convergent retinotectal connections on a single tectum neuron. We found that repetitive correlated spiking of pre- and postsynaptic neurons can result in persistent synaptic potentiation or depression, depending on the temporal order of the activity among various synaptic inputs. A synaptic input becomes potentiated if it is repetitively activated within 20 ms before spiking of the postsynaptic neuron, and becomes depressed if it is repetitively activated within 20 ms after postsynaptic spiking. These findings indicate the importance of the temporal order of synaptic activation among convergent inputs and set a stringent constraint on the effective pattern of retinal inputs for the refinement of developing retinotectal connections.

Retinotectal projection in developing brain

Whole-cell perforated patch recordings[15,16] were made from tectal neurons after surgical exposure of the inner surface of the tectum in *Xenopus* tadpoles (stage 40–41). Extracellular stimulation was applied to the surface of the contralateral retina by two loose-patch electrodes after removal of the lens (Fig. 1a). Evoked excitatory postsynaptic currents (EPSCs) were mediated by the AMPA (α-amino-3-hydroxy-5-methyl-4-isoxazole propionic acid) subtype of glutamate receptors, as they were abolished by 6-cyano-7-nitroquinoxaline-2,3-dione (CNQX, Fig. 1b). Polysynaptic responses

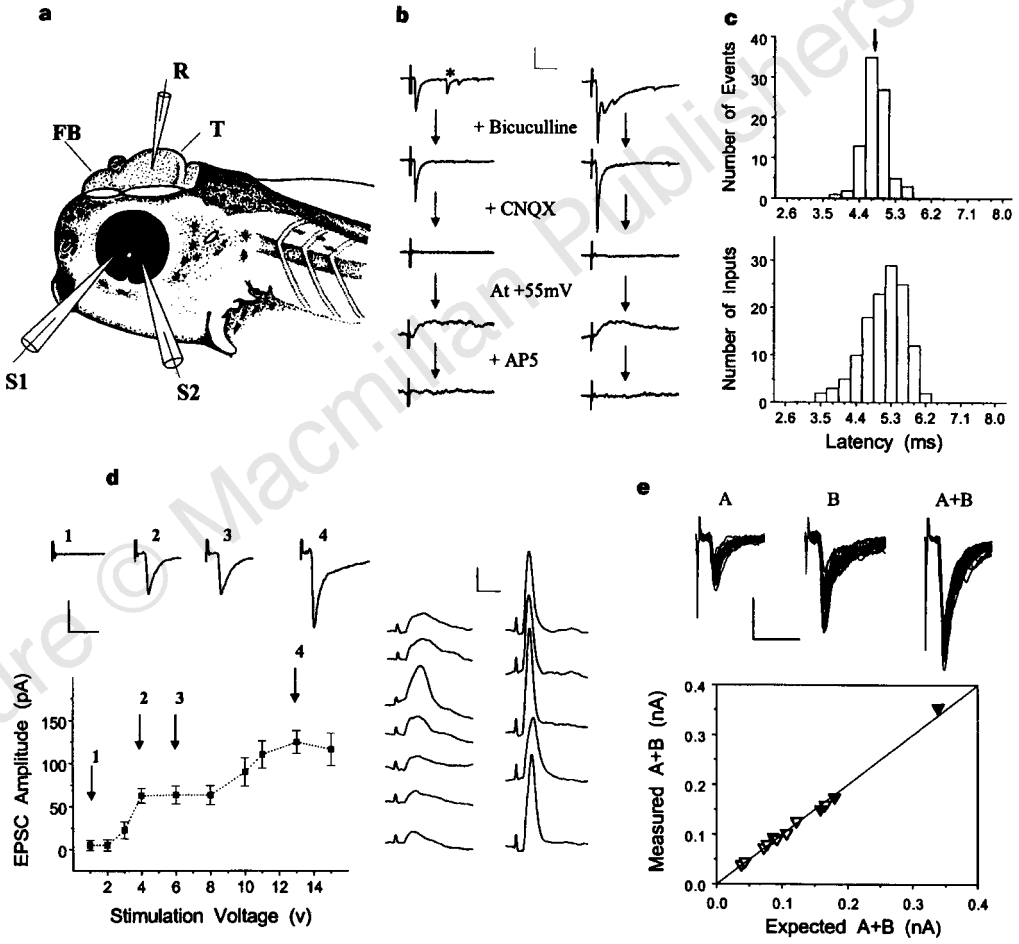

Figure 1 *In vivo* whole-cell recording from *Xenopus* tadpole brain. **a**, Recording arrangement. R, recording electrode; T, tectum; FB, forebrain; S1 and S2; extracellular stimulation electrodes. **b**, Typical evoked synaptic currents recorded in the tectal cell ($V_h = -70$ mV). Left: majority events, a single fast inward current with an onset latency of about 5 ms. Right, minority events, a fast inward current followed by a slow inward current. Each trace is an average of 4 consecutive events; the asterisk marks spontaneous activity. Recordings are from the same cell following sequential addition of bicuculline (10 μM), CNQX (10 μM) and AP5 (50 μM) as indicated, with V_h changed to +55 mV following the CNQX treatment. Scale bars: 30 pA, 25 ms. **c**, Latency of onset of EPSCs. Latency was defined as the time between the onset of 1-ms stimuli and the synaptic current. Top, latency distribution for EPSCs recorded from a tectal cell (arrow marks the mean). Bottom, distribution of the mean latency of a large population of synaptic inputs ($n = 129$). **d**, Dependence of the EPSC amplitude on the stimulus intensity. Data are amplitudes of EPSCs (mean ± s.e.m.) induced by stimulation at different voltages, including failures. Arrows 3 and 4 mark the level of 'minimal' and 'non-minimal' stimulation, respectively. Top, average of 10 consecutive events. Scale bars: 50 pA, 15 ms. Right, consecutive traces of the membrane-potential change of the tectal cell following 'minimal' (left) and 'non-minimal' (right) stimulation, respectively. (Scale bars: 15 mV, 15 ms). **e**, Traces are of 15 superimposed, consecutive EPSCs in a tectal neuron evoked by stimulating either one or two converging retinal inputs (A or B) and by co-stimulation of both inputs (A + B), as indicated. Scale bars: 50 pA, 20 ms. The graph shows corresponding values of the calculated sum of mean EPSC amplitudes obtained from separate stimulation (expected A + B) and of measured amplitudes of EPSCs evoked by synchronous co-stimulation of both inputs (measured A + B). Each point represents recording from one tectal cell. Data are from 'minimal' (open symbols) and 'non-minimal' (filled symbols) stimulation, respectively.

observed in some neurons were abolished by bicuculline, indicating the presence of inhibitory postsynaptic currents (IPSCs) mediated by $GABA_A$ (γ-aminobutyric acid A) receptors (Fig. 1b). Consistent with previous reports[17,18], these retinotectal synapses contain NMDA (*N*-methyl-D-aspartate) receptors, which were revealed by the appearance of outward EPSCs at V_h of +55 mV after CNQX treatment and the sensitivity of the latter currents to (D)-2-amino-5-phonovaleric acid (AP5; Fig. 1b). Here we considered EPSCs that had a latency of onset in the range of 3.5 to 6.5 ms following retinal stimulation; these are likely to be monosynaptic in nature. Figure 1c shows the distribution of the latency for EPSCs recorded from a typical tectal cell and the distribution of the mean latency for a population of tectal cells studied.

In most experiments, 'minimal' stimulation was used to stimulate the retinal neuron. The stimulus strength was increased in small increments from a low level. EPSCs usually appeared at a threshold stimuli and the mean amplitude remained constant afterwards over a relatively wide range of stimulus intensity (see Fig. 1d). The intensity of the 'minimal' stimulation was set to about 120–150% of the threshold, where a stable 'minimal' EPSC was evoked, consistent with the activation of one or a few neurons. In current clamp, 'minimal' stimulation usually elicited subthreshold evoked potentials (Fig. 1d), although in some cases it was capable of initiating spiking of the tectal neuron. In some experiments, the stimulus intensity was further increased to a level that consistently induced spiking of the tectal cell (Fig. 1d). The latter 'non-minimal' stimulation was likely to activate multiple retinal neurons. Anatomical studies have shown that the projection of single retinal ganglion cell axons in stage 40–41 *Xenopus* tadpoles extends to a large portion of the tectal neuropile[19,20]. Indeed, EPSCs could be recorded sequentially from several tectal cells along the rostral–caudal axis of the tectum when the same stimulation was applied to the same retinal site (data not shown). When the retina was stimulated at two sites 50–150 μm apart on the nasal and temporal sides of the optic head (a stimulation configuration we used as standard in this study), there was a relatively high frequency of observing convergent retinal inputs onto a single tectal cell. The evoked responses elicited by two convergent retinal inputs were fully additive, as would be expected if the stimulating electrodes were activating separate populations of retinal ganglion cells (Fig. 1e).

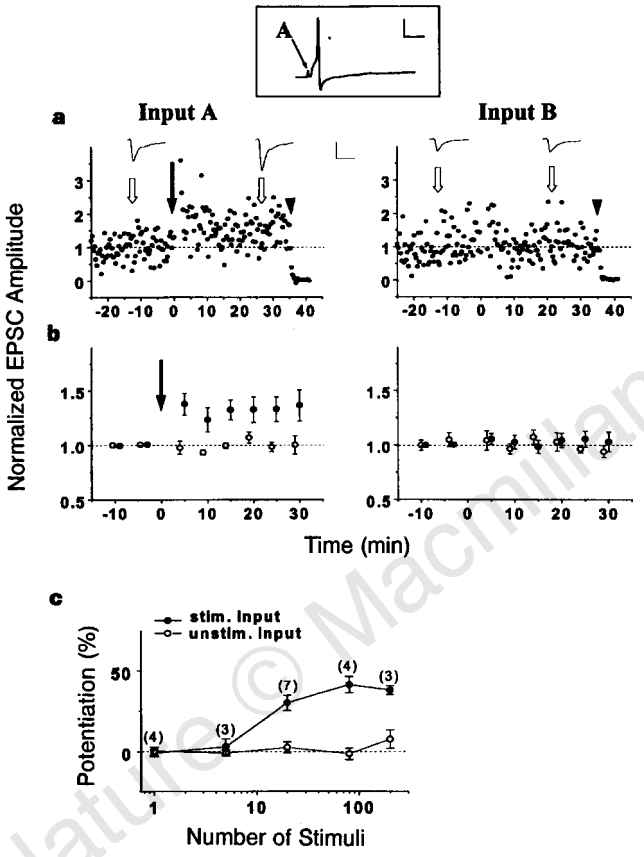

Figure 2 Effects of repetitive stimulation of one of two convergent retinal inputs. **a**, Amplitude of EPSCs elicited by test stimuli (0.063 Hz) at the repetitively stimulated input (A) and unstimulated input (B), respectively, normalized by the mean value observed before repetitive stimulation (dotted line). Sample EPSC traces are the average of 15 consecutive events at the time marked by the arrow. Scale bars: 50 pA, 10 ms. Repetitive stimulation (1 Hz for 20 s at time '0') was applied to input A, resulting in consistent spiking of the tectal cell (in current-clamp, see box; scale bars: 20 mV, 20 ms). Arrowhead indicated CNQX application (10 μM). **b**, Summary of results from all experiments similar to that shown in **a**. Normalized EPSC amplitudes from each experiment are averaged over 6-min bins before and 5-min bins after repetitive stimulation. Filled circles indicate experiments ($n = 7$) in which the stimulated input A was suprathreshold. The change in the mean EPSC amplitude at the input A 10–30 min after repetitive stimulation (compared with mean pre-stimulation values) was 32 ± 10% (s.e.m., $n = 7$), whereas that of unstimulated input B was 0.2 ± 6%. Open circles indicate experiments ($n = 4$) in which the stimulated input A was subthreshold (points laterally displaced to the left for clarity). **c**, Dependence of synaptic potentiation on the total number of repetitive stimuli. Potentiation is defined as the percentage increase (mean ± s.e.m.) in EPSC amplitude 10–30 min after repetitive stimulation. Data are for stimulated (filled circles) and unstimulated (open circles) inputs after different numbers of repetitive stimuli were applied (at 1 Hz). The number of experiments performed is shown in the parenthesis.

Repetitive stimulation of single inputs

By recording from tectal neurons innervated by two convergent inputs from nasal and temporal parts of the retina, we examined the effect of repetitive stimulation of one of the retinal inputs. The

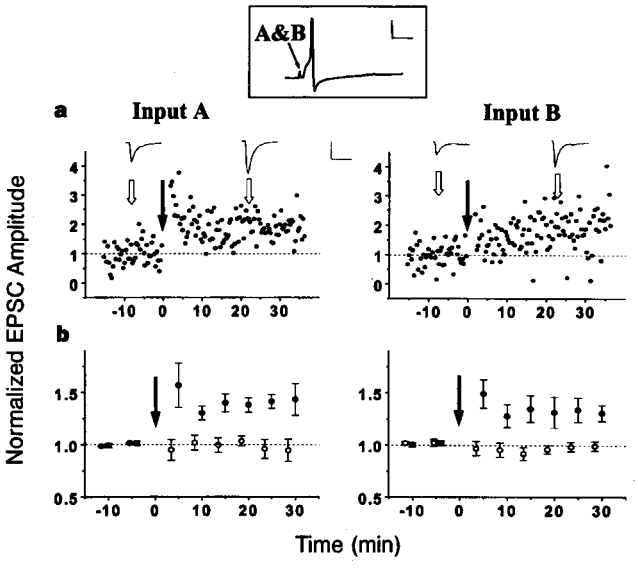

Figure 3 Effects of repetitive synchronous co-stimulation of two convergent retinal inputs. Action potentials were initiated in the tectal cell during repetitive co-stimulation (1 Hz for 20 s). **a**, Results from an experiment in which input A was suprathreshold and input B was subthreshold. **b**, Results from 7 synchronous co-stimulation experiments in which postsynaptic spiking was induced (filled circles). The change in the mean amplitude of EPSCs 10–30 min after repetitive stimulation was 36 ± 7% (s.e.m., $n = 7$) and 29 ± 10% (s.e.m.) at inputs A and B, respectively. Open circles show results from 3 experiments in which synchronous co-stimulation did not result in postsynaptic spiking. Scale bars as Fig. 2.

synaptic strength was assayed by measuring the amplitude of EPSCs of each retinal input (A or B) at a low stimulation frequency (0.063 Hz). During the repetitive stimulation of input A (1 Hz for 20 s), the tectal neuron was held in current clamp and action potentials were consistently initiated. As shown in Fig. 2a, the mean EPSC amplitude of input A was increased immediately after the repetitive stimulation of input A, whereas that of the unstimulated input B remained unchanged. Thus repetitive stimulation had resulted in homosynaptic potentiation of the stimulated input without affecting the unstimulated input converging onto the same tectal neuron. A summary of results from seven experiments is shown in Fig. 2b. In a different set of experiments, in which the repetitively stimulated inputs were subthreshold, we found no detectable change in both inputs (Fig. 2b). Thus spiking of the tectal neuron appears to be necessary for the induction of synaptic potentiation by the present protocol. In dually innervated *Xenopus* myocytes, repetitive stimulation of one input was found to induce persistent heterosynaptic depression of the other unstimulated input[21], a phenomenon that appears to be absent in this retinotectal system.

To examine further the dependence of synaptic potentiation on the pattern of stimulation, we varied the total number and frequency of repetitive stimuli. The degree of potentiation at the stimulated suprathreshold input increased with an increasing number of stimuli (at 1 Hz) and reached a plateau value at about 80 stimuli (Fig. 2c). No significant change in synaptic strength was observed at unstimulated subthreshold inputs in any of the conditions tested (up to 200 stimuli). Because the unstimulated input was not affected in these experiments following repetitive spiking of the postsynaptic neuron, postsynaptic spiking by itself appears to be insufficient to cause synaptic potentiation. Furthermore, we found that the potentiation effect did not depend on the frequency of

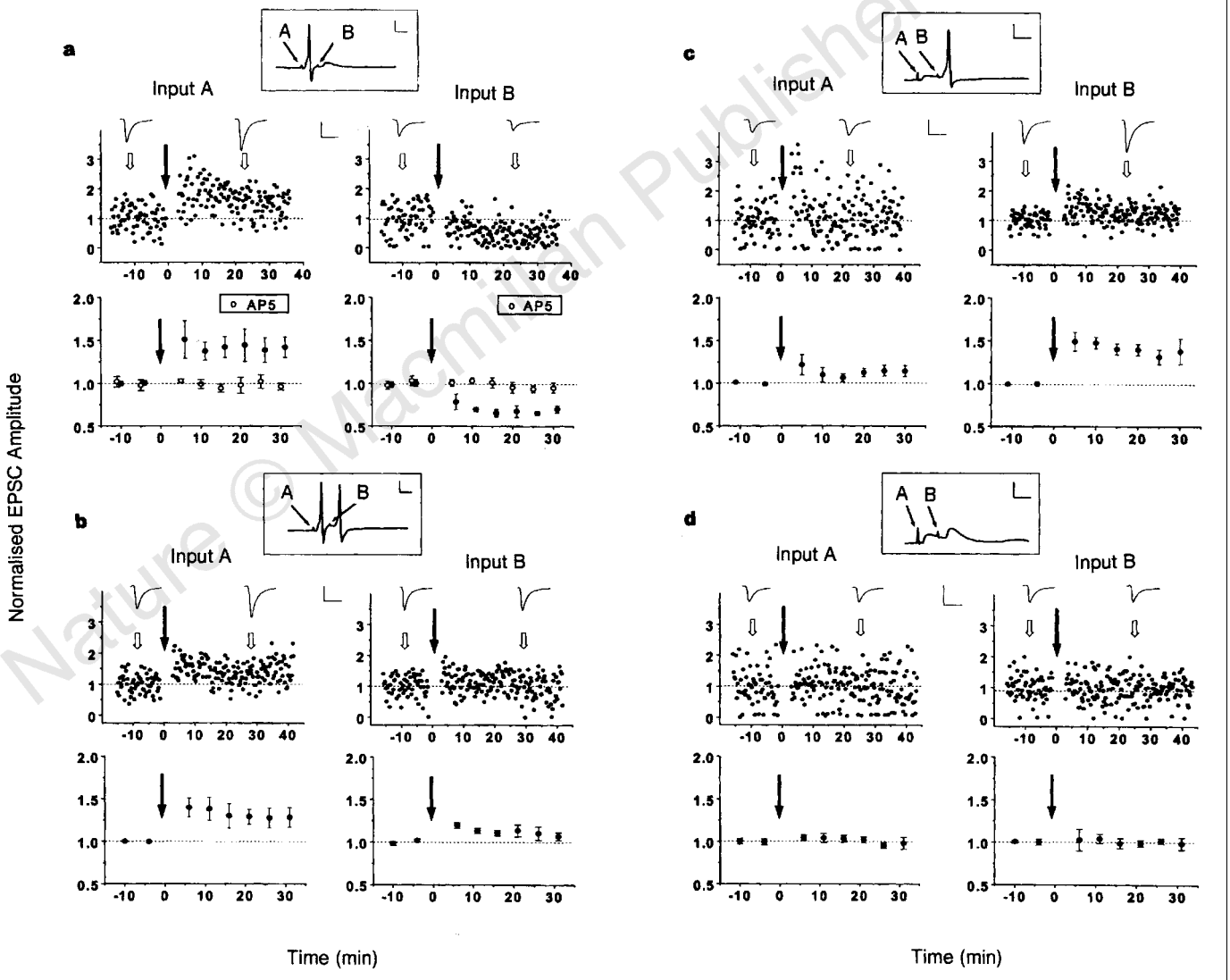

Figure 4 Effects of repetitive asynchronous co-stimulation of two convergent retinal inputs. **a**, Top, examples of synaptic changes induced at two convergent inputs on a tectal cell following repetitive co-stimulation (at time '0', 1 Hz for 100 s), with input A (suprathreshold) stimulated 15 ms before input B (subthreshold), with the tectal cell held in current clamp (see boxed trace; average of 5 events; scale bars: 20 mV, 15 ms). Bottom, results from all 6 experiments similar to that shown above (filled symbols). Note potentiation of input A (40 ± 10%, $n = 6$) and depression of input B (− 33 ± 4%, $n = 6$). Open symbols show results from 4 experiments identical to that in **a** but with AP5 (50 μM) added to the recording medium. **b**, Same as that in **a** except that both inputs were suprathreshold. Note the marked potentiation of input A (35 ± 9%, $n = 5$) and much weaker potentiation of input B (13 ± 3.6%, $n = 5$) following the repetitive stimulation. **c**, As **a**, except that input A was subthreshold and input B was suprathreshold. Note the marked potentiation of input B (42 ± 7%, $n = 5$) and weaker potentiation of input A (13 ± 4.5%, $n = 5$). **d**, As **a**, except that both inputs were subthreshold. No change in synaptic strength was observed at either input A (1.1 ± 4%, $n = 4$) or input B (0.8 ± 4%, $n = 4$).

stimulation. Application of 100 stimuli at 1, 5 and 20 Hz or of 150 stimuli in theta burst pattern resulted in a similar extent of potentiation of the stimulated input (data not shown). Thus 1 Hz was chosen for our standard stimulation protocol.

Synchronous co-stimulation of convergent inputs

To investigate the issue of synaptic interactions between convergent retinal inputs on a single tectal cell, we examined the effect of repetitive synchronous co-stimulation of both retinal inputs. As shown in Fig. 3a, the amplitude of EPSCs was increased at both inputs following repetitive co-activation for 20 stimuli at a frequency of 1 Hz. In this experiment, input A was suprathreshold, whereas input B was subthreshold. In other experiments, we found similar potentiation of both inputs when both inputs were subthreshold, as long as postsynaptic spiking was consistently initiated. For the seven experiments shown in Fig. 3b, both inputs were subthreshold in two cases (but initiated spiking when co-activated), but in five cases only input B was subthreshold. In two other experiments, in which both inputs were suprathreshold, both inputs became potentiated after repetitive co-stimulation (data not shown). Thus a subthreshold synaptic input became strengthened when it was activated synchronously with a suprathreshold input, but no change was observed if it was not stimulated (Fig. 2b). Consistent with that found for the repetitive stimulation of single inputs, no potentiation of either input was observed when synchronous co-stimulation produced only subthreshold synaptic potential in the tectal cell (Fig. 3b).

Asynchronous co-stimulation of convergent inputs

The effect of temporal pattern of activity on synaptic interactions between converging inputs was explored further by a series of studies using repetitive asynchronous co-stimulation. In the first set of experiments, the first input (A) elicited spiking in the tectal cell, whereas the second input (B), 15 ms later, resulted in only subthreshold EPSPs (Fig. 4a). After 100 paired stimuli at 1 Hz, input A became potentiated and input B became depressed; results from six experiments are summarized in Fig. 4a. In the second set of experiments, both inputs A and B were capable of initiating spiking of the tectal neuron. After the same 100 paired stimuli, input A was markedly potentiated, whereas input B exhibited only a slight potentiation (Fig. 4b). Taken together with the data shown in Fig. 4a, these results suggest that the suprathreshold input B can protect itself from depression induced by the preceding suprathreshold input A. The limited potentiation of input B may be attributed to the depressive effect of the spiking induced by input A. In the third set of experiments, in which the tectal response to input A was subthreshold and input B initiated spiking, input B showed substantial potentiation following repetitive co-stimulation, whereas the potentiation of input A was rather limited (Fig. 4c). In the latter case, the onset of the synaptic response to input A was about 20 ms before the peak of the spike induced by input B, although the interval between the stimuli applied at the retina was 15 ms. Finally, when both inputs were subthreshold, repetitive asynchronous co-stimulation produced no significant effect on the synaptic efficacy of either input (Fig. 4d). These results confirm that postsynaptic spiking is required for the induction of synaptic potentiation. Furthermore, persistent synaptic depression is induced when the subthreshold input is activated within 15–20 ms after spiking of the postsynaptic neuron. Finally, although synaptic potentiation was induced at a subthreshold input when it was activated immediately before postsynaptic spiking (as synchronous co-activation), the potentiation effect largely disappeared when the subthreshold input was activated about 20 ms before the peak of the postsynaptic action potential.

Timing requirements for synaptic modifications

The precise timing of synaptic activation required for the induction of synaptic potentiation or depression was examined further by varying the time interval between the stimuli repetitively applied to the two converging inputs. We considered the situation illustrated in Fig. 4a, c, in which one retinal input initiated postsynaptic spiking while the other was subthreshold. We varied the interval from −100 to 100 ms and determined the degree of synaptic potentiation or depression for the subthreshold input 10–30 min after the repetitive paired stimulation. Plotting the percentage change in the mean EPSC amplitude with the onset time of the synaptic potential relative to the peak of the action potential elicited in the tectal cell (Fig. 5) allowed us to identify distinct windows for the induction of potentiation and depression. Synaptic potentiation was found for inputs that repetitively arrived within 20 ms before the peak of the action potential, and depression was found for those repetitively arriving within 20 ms after the peak of the action potential. A transition between maximal potential and maximal depression occurs with only a 10-ms change in the timing of the synaptic input.

Cellular mechanisms

Activation of NMDA receptors is required for activity-dependent segregation of retinal axons into eye-specific stripes in frog transplanted with a third eye[22] and for the refinement of the topographic map[23,24]. Activity-induced long-term potentiation (LTP) and depression (LTD) in the CA1 region of the hippocampus[25,26] and in the visual cortex[27–29] and lateral geniculate nucleus (LGN)[30,31] have also been shown to depend on the activation of NMDA receptors. Here we have added AP5 (50 μM), a selective NMDA receptor antagonist, to the perfusion medium. This treatment did not affect the spiking of the tectal neuron. However, we found that asynchronous paired stimulation similar to that described above for

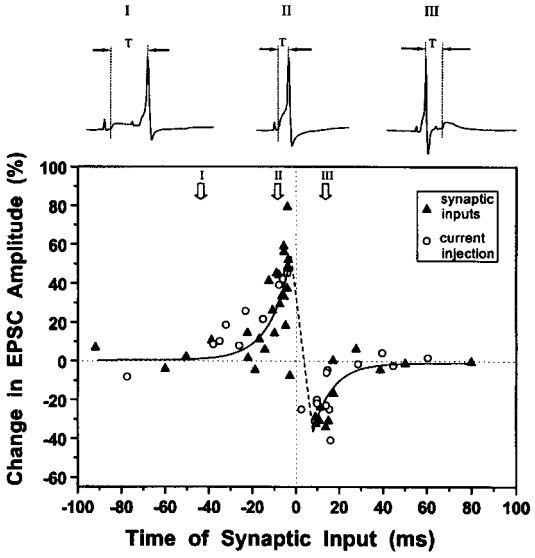

Figure 5 The critical window for synaptic potentiation and depression. The percentage change in the EPSC amplitude of synaptic inputs 10–30 min after repetitive stimulation was plotted against the time of the input (defined by the onset time of the EPSP relative to the peak of the action potential initiated in the tectal cell). Filled triangles show data from experiments similar to those described in Fig. 4a, c. Two converging inputs (one suprathreshold and one subthreshold) were stimulated repetitively (at 1 Hz for 100 s), with varying intervals between the stimuli applied to the two inputs. Only changes in the strength of the subthreshold input were plotted. The results for synaptic inputs were fitted separately for positive and negative times with first-order kinetics, as shown by solid curves. Open circles show data from experiments in which repetitive spiking (at 1 Hz for 100 s) of the tectal cell was induced by injections of depolarizing currents at different times with respect to a subthreshold synaptic input.

Fig. 4a was ineffective in modifying the synaptic strength at either input. The results from five experiments are shown in Fig. 4a. Thus activation of NMDA receptors (see Fig. 1b) is required for the induction of persistent synaptic modification at retinotectal synapses.

Studies of rat brain slices have shown that back-propagated action potentials initiated in the postsynaptic neuron by current injection at the soma exert a critical influence on the strength of synaptic inputs at dendrites[32–34]. The synaptic input became potentiated when it was activated repetitively 10 ms before the action potential, and was depressed if activated repetitively 10 ms after the action potential[32]. Our data show that action potentials initiated by synaptic inputs are effective in inducing synaptic modification, and that there is a narrow time window for the induction of potentiation or depression. To further test the sufficiency of postsynaptic spiking in inducing synaptic modifications in this system, we applied brief (1 ms) depolarizing currents into the tectal cell (in current clamp) to initiate repetitive spiking at different times before and after the onset of EPSPs evoked by a subthreshold retinal input. After 100 paired pre- and postsynaptic stimuli at 1 Hz, changes in synaptic efficacy were measured. As shown in Fig. 5, the degree of synaptic potentiation or depression depends critically on the time of onset of EPSPs with respect to the action potentials induced by the current injection, in a manner similar to that found for spiking induced by synaptic inputs. Thus spiking of tectal neuron is a sufficient postsynaptic condition for the induction of synaptic modifications. Furthermore, postsynaptic spiking is necessary for the induction of potentiation at suprathreshold inputs induced by repetitive synaptic activation, as voltage clamping the tectal cell at −70 mV during repetitive stimulation of suprathreshold inputs (1 Hz, 100 s) prevented the induction of potentiation. The percentage change in EPSC amplitude at 10–30 min post-stimulation was $0.1 \pm 4.1\%$ ($\pm$ s.e.m., $n = 4$), but was $41 \pm 11\%$ ($n = 9$) when repetitive stimulation was applied in the current-clamp condition. Finally, we examined the involvement of NMDA receptors in synaptic modifications induced using correlated postsynaptic current injections. For spiking repetitively induced within 20 ms after the onset of synaptic response, the changes in the EPSC amplitude were $-1.5 \pm 4.9\%$ ($n = 4$) in the presence of AP5 (50 μM) and $39 \pm 8.0\%$ ($n = 4$) without AP5. For spiking induced within 20 min before the onset of synaptic response, the changes were $4.5 \pm 2.5\%$ ($n = 4$) and $-23 \pm 9.8\%$ ($n = 7$) in the presence and absence of AP5, respectively. These results further support the idea that the same induction mechanism underlies the modification induced by either synaptic inputs or current injections.

The 'depression window' roughly coincides with the after-hyperpolarization following the action potential in the tectal neuron. We tested the possibility that hyperpolarization itself induces depression of a subthreshold input by using hyperpolarization induced by direct injection of negative current. As shown in Fig. 6a, induced hyperpolarization in synchrony with repetitive activation of a subthreshold input had no effect on synaptic strength, but the same input was later depressed significantly when repetitive synaptic activation was preceded by spiking of the tectal neuron induced by repetitive injection of positive currents. In five experiments, the change in the EPSC amplitude averaged $3.1 \pm 5.0\%$ following repetitive synaptic activation in the presence of hyperpolarization, indicating that hyperpolarization by itself is not sufficient for inducing depression in the subthreshold input. The following experiments further confirmed the critical importance of postsynaptic spiking. The spiking of tectal cells induced by suprathreshold inputs was prevented by injections of hyperpolarizing currents during repetitive retinal stimulation. We found that this procedure blocked synaptic potentiation at the suprathreshold input ($-1.3 \pm 2.5\%$, $n = 4$; see Fig. 6b). Furthermore, in the case of asynchronous co-stimulation of two suprathreshold inputs (interval 15 ms), hyperpolarizing currents that repetitively blocked spiking induced by the second input resulted in depression of the latter ($-25 \pm 4.4\%$, $n = 4$; see Fig. 6c). The same synapse showed potentiation following repetitive stimulation in the absence of induced hyperpolarization. In the case of asynchronous co-stimulation of two subthreshold inputs (interval 15 ms), hyperpolarization of the tectal cell during repetitive stimulation of the second input produced no effect on the synaptic efficacy of either input (data not shown). Thus inhibitory inputs, by hyperpolarizing the tectal cell, may serve to modulate interactions between excitatory synapses.

Discussion

Our results indicate that persistent synaptic modifications in the developing retinotectal system are determined both by the temporal

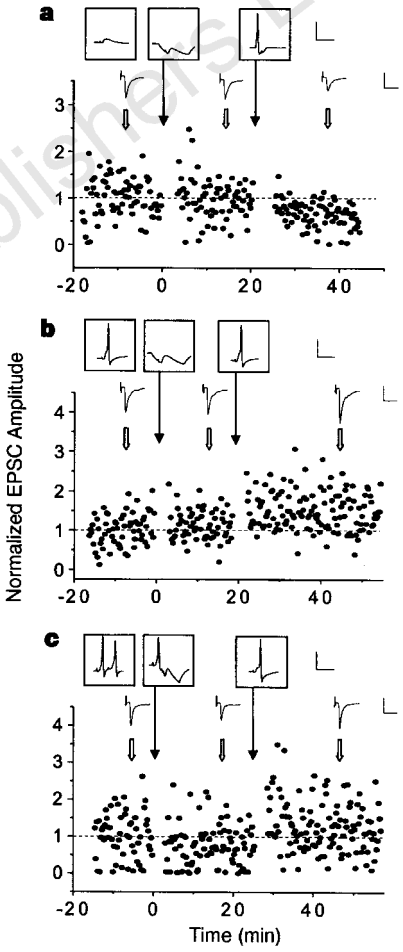

Figure 6 Effects of postsynaptic hyperpolarizations. **a**, Hyperpolarizations (20 mV) were induced in the tectal cell (in current clamp) by injections of negative currents (50 ms duration) in synchrony with repetitive stimulation of a subthreshold input. Boxes above the graphs show sample evoked potentials (average of 5 events; scale bars: 40 mV, 30 ms) during the test period (left) and during repetitive stimulation (black arrows; 1 Hz for 100 s). Lower traces show sample EPSCs (average of 15; scale bars: 30 pA, 20 ms). During the second episode of repetitive stimulation, spiking was initiated repetitively 10 ms before the presynaptic stimulation by injecting depolarizing currents (2 ms). **b**, Hyperpolarizations (25 mV) in synchrony with repetitive stimulation of a suprathreshold input. The postsynaptic spiking was abolished by hyperpolarization (middle box) during the first but not the second episode of repetitive stimulation. **c**, Repetitive hyperpolarizations (40 mV) in synchrony with the second of the two asynchronously activated suprathreshold inputs (with an interval of 15 ms). The blockade of the spiking induced by the second input (middle box) led to depression of the latter. Further repetitive stimulation of the second input alone, in the absence of hyperpolarizations (right box), led to potentiation of the same input.

order of activation of convergent retinal inputs and by their initial synaptic strength. Suprathreshold input that elicits spiking by itself appears to have a competitive advantage among converging inputs, because the onset of its EPSPs is always within the 'potentiation window' preceding the spiking of the postsynaptic neuron. For a subthreshold input, the timing of repetitive activation with respect to other inputs becomes critical in determining its fate: arrival within a 20-ms 'potentiation window' before postsynaptic spiking initiated by other inputs leads to potentiation, whereas arrival within a 20-ms 'depression window' after spiking leads to depression. Suprathreshold inputs can therefore help to strengthen preceding or synchronously activated subthreshold inputs, but can weaken them by initiating spiking immediately before their activation. Subthreshold inputs may cooperate by initiating spiking of the postsynaptic neuron through synchronous co-activation. Among convergent suprathreshold inputs, the input that is repetitively activated earlier than others wins in competition. As shown by the finding that induction of spiking within 20 ms following a preceding spike resulted in a reduced potentiation effect (Fig. 4b), the depression window also seems to apply to suprathreshold inputs. Finally, the effect of hyperpolarization shown in Fig. 6 suggests that convergent inhibitory inputs that are repetitively co-activated synchronously with a suprathreshold input may render the latter a disadvantageous position in synaptic competition, because blocking postsynaptic spiking by hyperpolarization prevents activity-induced potentiation of the suprathreshold input. Thus a retinal input that results in monosynaptic EPSCs followed by one or more polysynaptic GABA-mediated currents (see Fig. 1b), which was observed in 30% of tectal cells recorded, is likely to win in synaptic competition. Local inhibitory circuits established early within the tectum may play an important part in the refinement of retinotectal map.

Increasing the cytosolic Ca^{2+} concentration is known to be critical in the induction of synaptic modification at many synapses[25,26,35]. It has been suggested that back-propagated action potentials can interact with NMDA receptors to trigger synaptic modifications through Ca^{2+} influx[32–34]. The critical time windows we have observed may be accounted for by the spatiotemporal pattern of Ca^{2+} elevation in the tectal neuron, resulting from a specific temporal sequence of opening of voltage-dependent Ca^{2+} and NMDA channels. We noted that spiking initiated by a second suprathreshold input does not erase the depressive effect of the first input (see Fig. 4b). Rather, the heterosynaptic depression induced by the first input appears to have reduced the homosynaptic potentiation resulting from the second input.

Of particular relevance to the formulation of Hebb's rule[36–43], our results indicate that completely uncorrelated activity and correlated activity of subthreshold inputs that fail to initiate postsynaptic spiking are ineffective in inducing synaptic modifications. Both potentiation and depression depend on correlated pre- and postsynaptic spiking but they require opposite temporal orders in the timing of spikes in the pre- and postsynaptic neurons. This asymmetry in the dependence on the timing of synaptic inputs may be crucial for the synaptic modifications underlying the development and plasticity of neural circuits[44,45]. A potential mechanism for generating correlated and sequential activation of pre- and postsynaptic neurons is provided by spontaneous waves of activity in the prenatal mammalian retina, which has been shown to be important for segregation of eye-specific layers in LGN[46–48]. Propagation of waves across the retina leads to the sequential excitation of neighbouring ganglion cells with a defined delay, which may lead to modification of their inputs to a common postsynaptic tectal neuron. In the embryonic or early larval frog, as the visual scene sweeps across the retina it provides correlated and sequential activation of retinal ganglion cells.

During the maturation of the *Xenopus* retinotectal map, a gradual refinement of connections results in the projection of retinal axons to progressively more restricted populations of tectal cells. In the absence of activity or NMDA-receptor function, this refinement is abolished and axon arbors from retinal ganglion cells increase their spread over the tectum[23]. Functional modification of synaptic strength may be a prerequisite or a consequence of the morphological changes associated with the sharpening of the map. The finding that functional modification of synaptic efficacy precedes the removal of nerve terminals during synapse elimination in a developing neuromuscular system[49] suggests that the structural and functional plasticity of developing nerve connections may be causally related. Because the functional modification of retinotectal synapses and the structural refinement of the retinotectal map depend similarly on the activity and NMDA receptors, the precise activity pattern and timing requirement we observed may help to predict how visual inputs of specific patterns can shape the connectivity in the developing visual system. □

Methods

Xenopus laevis tadpoles were staged using the criteria of Nieuwkoop and Faber[50]. The stage 40–41 tadpole was secured by insect pins to a Sylgard-coated dish and incubated in HEPES-buffered saline containing (in mM): 115 NaCl, 2 KCl, 10 HEPES, 2.5 $CaCl_2$, 10 glucose, 1.5 $MgCl_2$, 0.005 glycine (pH 7.3). For recording from tectal cells, the skin on top of the head was removed and the brain was split open along the midline to expose the inner surface of the tectum on one side. The lens of the contralateral eye was removed to expose the surface of the retina. A low dose (1 $\mu g\,ml^{-1}$) of α-bungarotoxin was applied to the bath to prevent occasional twitching of muscle fibres during the recording. The toxin treatment did not affect retinotectal responses recorded. As shown in Fig. 1b, in the absence of α-bungarotoxin treatment, tectal responses recorded were account for entirely by glutamatergic and GABA-ergic transmission. Furthermore, in three experiments performed on tadpoles not treated with the toxin, we observed persistent activity-induced synaptic potentiation as well as synaptic depression, in a manner similar to that described in the text. Perfusion with 50 μM tubocurarine at the end of these experiments resulted in no significant change in both evoked and spontaneous activity.

The method of whole-cell perforated patch recording[15] was used to record from tectal cells, using amphotericin B (Sigma) for perforation[16]. The micropipettes were made from borosilicate glass capillaries (Kimax), with a resistance in the range 4–6 MΩ. The pipettes were coated with a layer of Sylgard except near the tip, and were tip-filled with internal solution and then back-filled with internal solution containing 200 $\mu g\,ml^{-1}$ of amphotericin B. The internal solution contained (in mM): 110 K-gluconate, 10 KCl, 5 NaCl, 1.5 $MgCl_2$, 20 HEPES, 0.5 EGTA (pH 7.3). The same patch pipette was used for stimulation of retinal neurons, except that the tip opening was increased to 3 μm, and the filling solution was the bath solution described above. The bath was constantly perfused with fresh recording medium at a slow rate throughout the experiment, and all experiments were performed at room temperature. Recordings were performed with a patch-clamp amplifier (Axopatch 1D; Axon Instruments). The series resistance (15–50 MΩ) was compensated at 75–85% (lag 60 μs). Signals were filtered at 5 kHz using amplifier circuitry and stored on a VCR. Data were sampled at 10 kHz and analysed using pClamp 6.0 software (Axon Instruments). Data accepted for analysis were cases where the average amplitude of EPSCs did not vary beyond 10% of the average value during the control period (15 min), the series resistance did not change by more than 10%, and input resistance (0.5–2 GΩ) remained relatively constant throughout the experiment. During the experiment, the spontaneous activity recorded in tectal cells was monitored continuously by a fast-transient chart recorder (Gould TA240). The stability of amplitude and frequency of spontaneous events was used as an indication of viability of the preparation. For assaying synaptic connectivity, the retinal neuron was extracellularly stimulated by 'blind' loose-patch at a low frequency (0.063 Hz) on the surface layer of the retina. Both EPSCs and IPSCs were inward currents at the clamping potential (−70 mV). The IPSCs have distinctly longer decay times and more negative reversal potentials than EPSCs. As shown in Fig. 1b, pharmacological studies indicated that EPSCs observed at negative membrane potentials are mediated by AMPA receptors, blocked by CNQX (10 μM, RBI). NMDA receptors are activated at positive membrane potentials and are blocked by the antagonist AP5 (50 μM,

RBI). IPSCs are mediated by $GABA_A$ receptors and blocked by bicuculline methiodide (10 μM, RBI). Owing to variation in the probability of initiating spiking of the tectal cell, experiments were carried out only on those synaptic inputs that were either strong enough to initiate spiking for most (>70%) stimuli (under either 'minimal' or 'non-minimal' stimulation) or rarely (< 10%) initiated spiking; these inputs are defined as 'suprathreshold' and 'subthreshold', respectively.

Received 15 May; accepted 29 June 1998.

1. Goodman, C. & Shatz, C. J. Developmental mechanisms that generate precise patterns of neuronal connectivity. *Cell* **72,** 77–98 (1993).
2. Katz, L. C. & Shatz, C. J. Synaptic activity and the construction of cortical circuits. *Science* **274,** 1133–1138 (1996).
3. Hubel, D. H. & Wiesel, T. N. The period of susceptibility to the physiological effects of unilateral eye closure in kittens. *J. Physiol. (Lond.)* **206,** 419–436 (1970).
4. LeVay, S., Hubel, D. H. & Wiesel, T. N. The development of ocular dominance columns in normal and visually deprived monkeys. *J. Comp. Neurol.* **191,** 1–51 (1980).
5. Stryker, M. P. & Harris, W. A. Binocular impulse blockade prevents the formation of ocular dominance columns in cat visual cortex. *J. Neurosci.* **6,** 2117–2133 (1986).
6. Shatz, C. J. & Stryker, M. P. Prenatal tetrodotoxin infusion blocks segregation of retinogeniculate afferents. *Science* **242,** 87–89 (1988).
7. Stryker, M. P. & Strickland, S. L. Physiological segregation of ocular dominance columns depends on the pattern of afferent electrical activity. *Invest. Ophthalmol. Vis. Sci.* **25, (Suppl.)** 278 (1984).
8. Weliky, M. & Katz, L. C. Disruption of orientation tuning in visual cortex by artificially correlated neuronal activity. *Nature* **386,** 680–685 (1997).
9. Udin, S. B. & Fawcett, J. W. Formation of topographic maps. *Annu. Rev. Neurosci.* **11,** 289–297 (1990).
10. Holt, C. E. & Harris, W. A. Position, guidance and mapping in the developing visual system. *J. Neurobiol.* **24,** 1400–1422 (1993).
11. Harris, W. A. The effects of eliminating impulse activity on the development of the retinotectal projection in salamanders. *J. Comp. Neurol.* **194,** 303–317 (1980).
12. Reh, T. A. & Constantine-Paton, M. Eye-specific segregation requires neural activity in three-eyed *Rana pipiens*. *J. Neurosci.* **5,** 1132–1143 (1985).
13. Schmidt, J. T. & Buzzard, M. Activity-driven sharpening of the retinotectal projection in goldfish: development under stroboscopic illumination prevents sharpening. *J. Neurobiol.* **24,** 384–399 (1993).
14. Brickley, S. G., Dawes, E. A., Keating, M. J. & Grant, S. Synchronizing retinal activity in both eyes disrupts binocular map development in the optic tectum. *J. Neurosci.* **18,** 1491–1504 (1998).
15. Hamill, O. P., Marty, A., Neher, E., Sakmann, B. & Sigworth, F. J. Improved patch-clamp techniques for high-resolution current recording from cells and cell-free membrane patches. *Pflugers Arch.* **391,** 85–100 (1981).
16. Rae, J., Cooper, K., Gates, P. & Watsky, M. Low access resistance perforated patch recordings using amphotericin B. *J. Neurosci. Methods* **37,** 15–26 (1991).
17. Wu, G.-Y., Malinow, R. & Cline, H. T. Maturation of a central glutamatergic synapse. *Science* **274,** 972–976 (1996).
18. Hickmott, P. W. & Constantine-Paton, M. The contribution of NMDA, non-NMDA, and GABA receptors to postsynaptic responses in neurons of the optic tectum. *J. Neurosci.* **13,** 4339–4353 (1993).
19. Sakaguchi, D. S. & Murphey, R. K. Map formation in the developing *Xenopus* retinotectal system: an examination of ganglion cell terminal arborizations. *J. Neurosci.* **5,** 3228–3245 (1985).
20. O'Rourke, N. A. & Fraser, S. E. Dynamic changes in optic fiber terminal arbors lead to retinotopic map formation: an *in vivo* confocal microscopic study. *Neuron* **5,** 159–171 (1990).
21. Lo, Y. & Poo, M.-m. Activity-dependent synaptic competition *in vitro*: Heterosynaptic suppression of developing synapses. *Science* **254,** 1019–1022 (1991).
22. Cline, H. T., Debski, E. & Constantine-Paton, M. N-methyl-D-aspartate receptor antagonists desegregates eye-specific stripes. *Proc. Natl Acad. Sci. USA* **84,** 4342–4345 (1987).
23. Cline, H. T. & Constantine-Paton, M. NMDA receptor antagonists disrupt the retinotectal topographic map. *Neuron* **3,** 413–426 (1989).
24. Schmidt, J. T. Long-term potentiation and activity-dependent retinotopic sharpening in the regenerating retinotectal projection of goldfish: common sensitive period and sensitivity to NMDA blockers. *J. Neurosci.* **10,** 233–246 (1990).
25. Bliss, T. V. & Collingridge, G. L. A synaptic model of memory: long-term potentiation in the hippocampus. *Nature* **361,** 31–39 (1993).
26. Malenka, R. C. Synaptic plasticity in the hippocampus: LTP and LTD. *Cell* **78,** 535–538 (1994).
27. Artola, A. & Singer, W. Long-term potentiation and NMDA receptors in rat visual cortex. *Nature* **330,** 649–652 (1987).
28. Komatsu, Y., Fujii, K., Maeda, J., Sakaguchi, H. & Toyama, K. Long-term potentiation of synaptic transmission in kitten visual cortex. *J. Neurophysiol.* **59,** 124–141 (1988).
29. Bear, M. F., Press, W. A. & Connors, B. W. Long-term potentiation in slices of kitten visual cortex and the effects of NMDA receptor blockade. *J. Neurophysiol.* **67,** 1–11 (1992).
30. Hahm, J. O., Langdom, R. B. & Sur, M. Disruption of retinogeniculate afferent segregation by antagonists to NMDA receptors. *Nature* **351,** 568–570 (1991).
31. Mooney, R., Madison, D. V. & Shatz, C. J. Enhancement of transmission at the developing retinogeniculate synapse. *Neuron* **10,** 815–825 (1993).
32. Markram, H., Lubke, J., Frotscher, M. & Sakmann, B. Regulation of synaptic efficacy by coincidence of postsynaptic APs and EPSPs. *Science* **275,** 213–215 (1997).
33. Magee, J. C. & Johnston, D. A synaptically controlled, associative signal for hebbian plasticity in hippocampal neuron. *Science* **275,** 209–213 (1997).
34. Debanne, D., Gähwiler, B. H. & Thompson, S. M. Long-term synaptic plasticity between pairs of individual CA3 pyramidal cells in rat hippocampal slice cultures *J. Physiol.* **507,** 237–247 (1998).
35. Naveu, D. & Zucker, R. S. Postsynaptic levels of $[Ca^{2+}]_i$ needed to trigger LTD and LTP. *Neuron* **16,** 619–629 (1996).
36. Hebb, D. H. *The Organization of Behavior* (Wiley, New York, 1949).
37. Stent, G. S. A physiological mechanism for Hebb's postulate of learning. *Proc. Natl Acad. Sci. USA* **70,** 997–1001 (1973).
38. Willshaw, D. J. & Von der Malsburg, C. How patterned neural connections can be set up by self-organization. *Proc. R. Soc. Lond. B* **194,** 431–445 (1976).
39. Bear, M. F., Cooper, L. N. & Ebner, F. F. A physiological basis for a theory of synaptic modification. *Science* **237,** 42–48 (1987).
40. Miller, K. D., Keller, J. B. & Stryker, M. P. Ocular dominance column development: analysis and simulation. *Science* **245,** 605–615 (1989).
41. Constantine-Paton, M., Cline, H. T. & Debski, E. Patterned activity, synaptic convergence, and the NMDA receptor in developing visual pathways. *Annu. Rev. Neurosci.* **13,** 129–154 (1990).
42. Brown, T. H., Kairiss, E. W. & Keenan, C. L. Hebbian synapses: biophysical mechanisms and algorithms. *Annu. Rev. Neurosci.* **13,** 475–511 (1990).
43. Frégnac, Y., Burke, J. P., Smith, D. & Friedlander, M. J. Temporal covariance of pre- and postsynaptic activity regulates functional connectivity in the visual cortex. *J. Neurophysiol.* **71,** 1403–1421 (1994).
44. Mehta, M. R., Barnes, C. A. & McNaughton, B. L. Experience-dependent, asymmetric expansion of hippocampal place fields. *Proc. Natl Acad. Sci. USA* **94,** 8918–8921 (1997).
45. Gerstner, W. & Abbott, L. F. Learning navigational maps through potentiation and modulation of hippocampal place cells. *J. Comp. Neurosci.* **4,** 79–94 (1997).
46. Meister, M., Wong, R. O., Baylor, D. A. & Shatz, C. J. Synchronous bursts of action potentials in ganglion cells of the developing mammalian retina. *Science* **252,** 939–943 (1991).
47. Wong, R. O., Chernjavsky, A., Smith, S. J. & Shatz, C. J. Early functional neural networks in the developing retina. *Nature* **374,** 716–718 (1995).
48. Penn, A. A., Riquelme, P. A., Feller, M. B. & Shatz, C. J. Competition in retinogeniculate patterning driven by spontaneous activity. *Science* **279,** 2108–2112 (1998).
49. Colman, H., Nabekura, J. & Lichtman, J. W. Alterations in synaptic strength preceding axon withdrawal. *Science* **275,** 356–361 (1997).
50. Nieuwkoop, P. D. & Faber, J. *Normal Table of* Xenopus laevis 2nd edn (North Holland, Amsterdam, 1967).

Acknowledgements. We thank G.-q. Bi, B. Berninger, Y. Dan, S. Mcfarlane and H. Cline for discussion and comments. This work was supported by grants from NIH, NSF and MRC.

Correspondence and requests for materials should be addressed to M.-m.P. (e-mail: mpoo@ucsd.edu).